aerospace

Communication

Examination and Prediction of the Lift Components of Low Aspect Ratio Rectangular Flat Plate Wings

Lance W. Traub

Aerospace Engineering Department, Embry Riddle Aeronautical University, Prescott, AZ 86301, USA; traubl@erau.edu

Abstract: An investigation of the lift components present over low aspect ratio rectangular wings is presented. Wing aspect ratios ranging from 0.5 to 3 are examined using published experimental results and analytic analysis methods. The methods are based on the fundamental decomposition of Polhamus; that is, lift is attributed to a potential flow lift component coupled with a vortical lift component stemming from the leading and side edges of the flat plate wing. The analysis suggests a low sensitivity to Reynolds numbers spanning three orders of magnitude and brings into doubt the realization of a leading edge vortex lift component for wings with unswept leading edges under steady state conditions. The analytic prediction method of Purvis is shown to provide close accord with all experimental data sets when lift contributions caused by a leading edge vortex are excluded.

Keywords: low aspect ratio wings; rectangular wings; drones; vortex lift; slender wings

check for updates

Citation: Traub, L.W. Examination and Prediction of the Lift Components of Low Aspect Ratio Rectangular Flat Plate Wings. *Aerospace* **2023**, *10*, 597. https://doi.org/10.3390/aerospace10070597

Academic Editor: Christian Breitsamter

Received: 9 May 2023
Revised: 26 June 2023
Accepted: 27 June 2023
Published: 30 June 2023

1. Introduction

Slender unswept wings can be used for various applications, ranging from missile control surfaces to more recent uses in small scale flight vehicles, i.e., drones and micro-aerial vehicles. As such, many studies have documented their performances [1–9]. These studies have shown that slender wings yield low lift curve slopes and low aerodynamic efficiency coupled with a delay in the stall angle compared to high aspect ratio wings. Polhamus [10] laid the foundation for the most successful approach to modeling these types of geometries. As the wings are typically thin and have extensive side edge length, their lift is assumed to be constituted of two components. The first is the attached potential flow lift which is generated due to the bound circulation over the wing in the absence of leading edge suction. The loss of leading edge suction yields an attached flow lift curve that is no longer linear with respect to angle of attack. The second component is the vortex lift, which is quantified using the so called "Leading Edge Suction Analogy", in which the leading edge or side edge suction force is effectively rotated by 90 degrees to the plane of the normal force. This assumes that a coherent vortex forms above the relevant surface and that flow re-attachment occurs inboard of that surface [10]. The vortex lift augments the attached flow potential lift and increases with the angle of attack.

Numerous comparisons validating this approach are present in the literature, especially with application to delta wings [3,10–15]. Slender rectangular wings have also been modeled using the leading edge suction analogy; with terms associated with vortex lift caused by the leading edge and side edges [3,11]. The lift curve for a slender rectangular wing is notably non-linear, indicative of the presence of lift associated with vortical action over the wing. The non-linearity of the lift curve tends to diminish as AR exceeds ≈ 1.5 to 2 [2,5]. Studies have shown the profound influence of the rolled up wing tip vortices: not only do they directly augment lift but the downwash field in-between the two tip vortices suppresses flow separation, yielding a significant increase in the stall angle. The detachment of the vortices at high angles of attack is associated with the onset of wing stall. Thorough the documentation of the application of the suction analogy to estimate side edge vortex lift is that of Lamar [11] and Lamar and Gloss [3], where numerous experiment and theory comparisons are reported. Using the approach of Refs. [3,11], a vortex lattice solver was utilized to establish the constants associated with potential and vortex lift. Torres and Mueller [5] applied the suction analogy to a series of low AR rectangular wings. However, the vortex lift constant (serving as a combination of vortex lift produced along the side edges and the leading edge) was set to π, while K_P was solved so as to maximize the agreement with experiment. Consequently, it is difficult to assess the applicability/accuracy of the method as it essentially devolves to a curve fit. Mitoguchi and Itoh [8] also applied Polhamus' lift decomposition, but in such a way as to solve the values of K_V and K_P, which agreed with the experiment using a least squares multiple regression. Consequently, this application of Polhamus' theory is also little more than a curve fit and does not explicitly validate the approach.

While the presence of side edge vortex lift is supported by flow diagnostics, which clearly show organized coherent vortical structures associated with the wing's lateral edges, the same is not evident for the leading edge. Flow visualization [8] shows the existence of large well defined tip vortices over low aspect ratio rectangular plates that when viewed in conjunction with force balance data are noted to significantly augment lift and delay stall though induced downwash. Surface pressure measurements [16] over an AR = 1 rectangular wing show distinct peaks in the pressure distribution adjacent to the wing tips reminiscent of those seen over delta wings—clear evidence of the tip vortices causing a side edge vortex lift contribution. As indicated in the literature [17,18], a lift-generating leading edge vortex can exist over unswept wings subject to unsteady motion. However, as the motion reaches steady state, the lift contribution due to the leading edge vortex rapidly diminishes as the vortical structure convects away from the wing. For a wing with zero leading edge sweep, separation will occur at the leading edge if it is sharp. The boundary layer, which is ostensibly laminar, separates and forms a bubble of the long type [19] after transients have died down and the flow reaches a steady state. Transition occurs rapidly in the shear layer as it is highly sensitive to disturbance, enabling flow re-attachment aided by the entrainment of the freestream. However, the measurements of surface pressure on thin flat plates [20] and thin diamond airfoils [21] do not show the typical manifestation of suction associated with a vortex (at least not on a time-averaged basis) in the vicinity of the leading edge; there are no localized peaks, just a flat plateau in the pressure trace commonly associated with separation. Consequently, the contribution of leading edge vortex lift to a rectangular wing under steady state conditions, as included in many documented studies, may be expedient in terms of data correlation but not realistic in terms of flow physics. Consequently, in this article, experimental data from the literature for low AR rectangular flat plate wings are compared and subsequently modeled using different formulations based on the leading edge suction analogy to assess the applicability of the models and the contribution of the leading edge vortex lift to the total lift.

2. Analytical Approach for Low Aspect Ratio Rectangular Wings

Following Polhamus [10], the lift of a thin, slender wing may be modeled as

$$C_L = K_P \cos(\alpha)^2 \sin(\alpha) + (K_{V-LE} + K_{V-SE}) \cos(\alpha) \sin(\alpha)^2 \quad (1)$$

The first term on the right hand side is the attached flow potential lift in the absence of leading edge suction. The second term is the vortex lift associated with the leading and side edges. K_P, the potential constant, is essentially the lift curve slope of the wing established at low angles of attack before any non-linear contributions are present. For a slender delta wing, $K_{V\text{-}LE}$ is often approximated as π; however, this value is not representative for rectangular wings. It may be found numerically, as outlined in Refs. [3,11]. Larson [7] developed analytic relations that essentially reproduce the coefficients described by Lamar using empirical modifications to Helmbold's equation [22] and lifting line theory estimated lift curve slopes. Larson's expressions for incompressible flow are summarized as Equations (2)–(4).

$$K_P = \frac{2\pi AR}{\left[2+\sqrt{(4/3)AR^2+4}\right]} \quad (2)$$

$$K_{V-LE} = \frac{\pi AR}{\left[2+\sqrt{(1/4)AR^2+4}\right]} \quad (3)$$

$$K_{V-SE} = \frac{2\pi}{[2+AR]} = \frac{\pi}{[1+AR/2]} \quad (4)$$

Equations (2) and (3) are recognizable as being based on Helmbold's [22] equation while Equation (4) stems from the lifting line theory. The constants of 4/3 and 1/3 were obtained by Larson as curve-fitting terms to fit Lamar's [11] expressions for K_P and $K_{V\text{-}LE}$.

Purvis [23] derived analytic expression to estimate leading edge and side edge vortex lift using an assumed load distribution over the wing. The load distribution was essentially that over a flat plate (stemming from thin airfoil theory) in the chordwise direction and varied elliptically spanwise. Relations derived by Purvis are shown as Equations (5) and (6).

$$K_{V-LE} = \left(K_P\cos(\alpha)^2 - \frac{{K_P}^2}{\pi AR}\cos(\alpha)^5\right)/\cos(\Lambda) \quad (5a)$$

If Equation (5a) is evaluated at low α, it reduces to Polhamus' [10] expression:

$$K_{V-LE} = \left(K_P - \frac{{K_P}^2}{\pi AR}\right)/\cos(\Lambda) \quad (5b)$$

For an unswept wing, cos(Λ) = 1. The side edge suction expression for a rectangular wing is given in [23] as:

$$K_{V-SE} = 4.91924\frac{{K_P}^2}{\pi AR^2}\cos(\alpha)^2 \quad (6)$$

and has been modified so as to be consistent with Purvis' formulation when incorporated into Equation (1). The value of the potential constant was not estimated by Purvis.

The potential constant may be assessed using any representative expression for the lift curve slope that is accurate for low AR. Examples include Helmbold's [22] original relationship

$$K_P = \frac{2\pi}{\left[\sqrt{1+(2/AR)^2}+(2/AR)\right]} \quad (7)$$

as well as Prandtl's lifting line equation (LLT) modified using Jones' edge perimeter correction [24]

$$K_P = \frac{2\pi}{[1+(3/AR)]} \quad (8)$$

where Jones' correction changes the original lifting line constant from 2 to 3 in the denominator. Hoerner and Borst [19] suggest a relationship of the form:

$$K_P = 180/[\pi(36.5/AR+2AR)] \quad (9)$$

Note that for thin sharp edge flat plates, the prediction of the drag coefficient due to lift is trivial and is simply given as

$$C_D - C_{Dmin} = C_L\tan(\alpha) \quad (10)$$

Consequently, an accurate C_L assessment will intrinsically yield an accurate estimation of the drag coefficient caused by lift.

3. Results and Discussion

Figure 1 summarizes estimates using Equations (2)–(9). As seen previously, predictions for K_P are close, with Larsen's [7] curve fit to Lamar's data [11] being functionally identical. Lamar's coefficients were determined numerically using a vortex lattice (VLM) code. Jones' edge correction to lifting line theory shows close accord with Lamar's results for AR > 1.5 but slightly overpredicts K_P below this AR. Conversely, Helmbold's equation shows close accord for AR < 1.5 and an increasing discrepancy with the VLM solution for AR > 1.5. The approximation of Hoerner and Borst [19] is also seen to show close agreement with Lamar's VLM estimates.

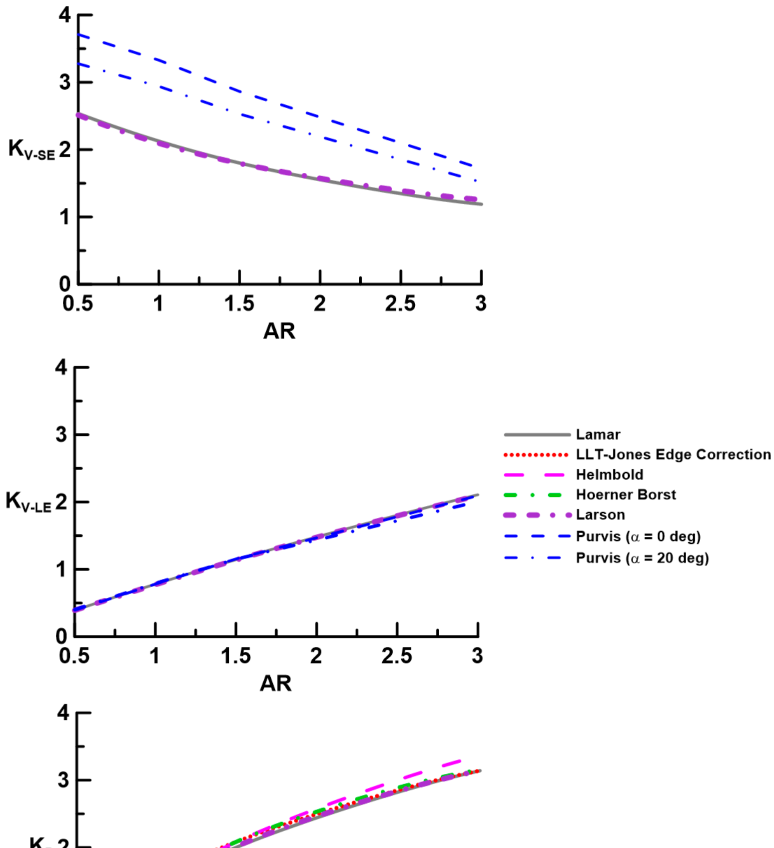

Figure 1. Coefficient estimates for the lift prediction of a rectangular wing.

The leading edge vortex lift constant ($K_{V\text{-}LE}$) is invariant between Lamar's VLM estimate and its functional curve fit following Larson. Estimates by Purvis [23] are α-dependent in their formulation; consequently, $K_{V\text{-}LE}$ values are given for $\alpha = 0$ and 20 degrees. Predictions by Purvis are seen to deviate slightly from those of Lamar/Larsen for AR > 1.5 at higher angle of attack ($\alpha = 20$ degrees), with a lower magnitude of leading edge vortex lift predicted. As may be expected due to the increasing lateral extent of the leading edge, $K_{V\text{-}LE}$ increases with AR.

The greatest discrepancy between the VLM estimates of Lamar and Purvis' analytic relationships is seen in $K_{V\text{-}SE}$. All estimates show a reduction in $K_{V\text{-}SE}$ with AR, a consequence of the reduction in the side edge extent compared to the wings perimeter. Purvis' estimates are notably higher than Lamar's and are also seen to show a significant dependency on α—increasing angle of attack decreases the value of $K_{V\text{-}SE}$.

Lift coefficient predictions are shown in Figure 2 for an AR = 0.5 flat plate. Experimental data sets spanning a range of Re are presented. The data sets show reasonable agreement for Re > 3000. Side edge vortex lift is seen to contribute the majority of the lift of the wings. Larson's predictions (equivalent to those of Lamar) yield reasonable agreement with experiment when all three lift components are included, i.e., potential lift as well as side edge and leading edge vortex lift. Purvis' C_L estimates shows closer accord with experiment than those of Larson when considering only the potential and side edge vortex lift; the addition of the leading edge vortex lift causes a slight overprediction. Note that to ensure a common reference for the comparison of Purvis' and Larson's (or Lamar's) methods, Equation (2) was used to estimate K_P for Purvis' results.

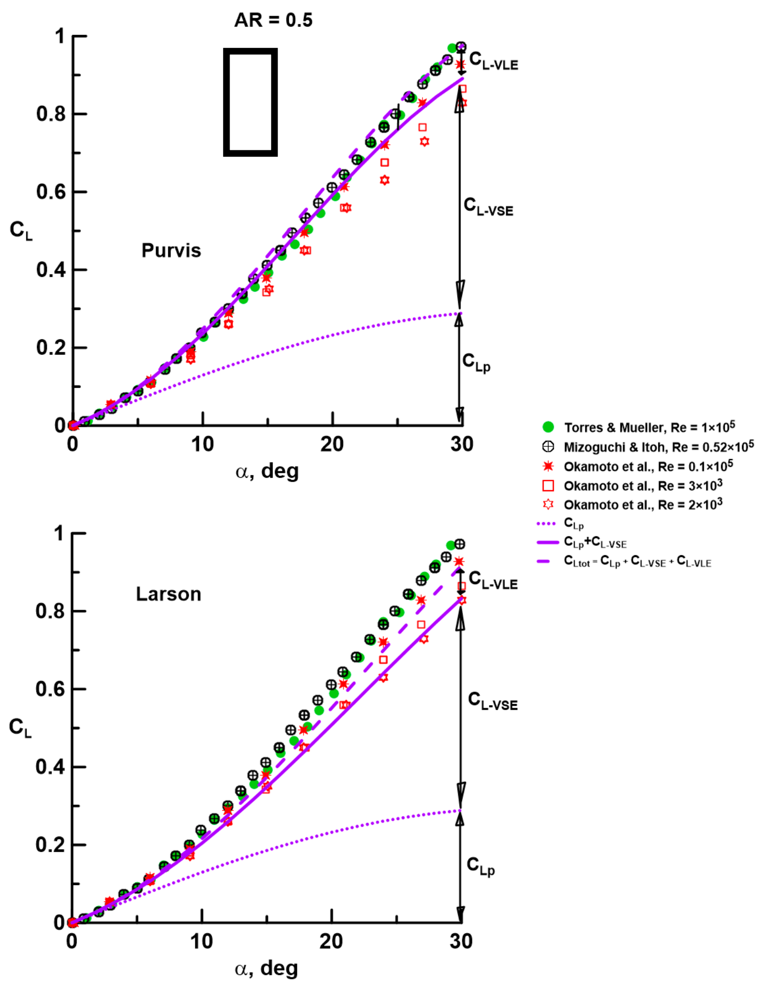

Figure 2. Lift coefficient correlation of methods of Purvis and Larson with experimental data for an AR = 0.5 rectangular flat plate wing. Okamoto et al. data from Ref. [2].

Increasing the plate's aspect ratio to 1 (see Figure 3) still shows a highly non-linear lift curve. Data sets are included that span a Reynolds number range of over three orders of magnitude: from 3000 to 2.16×10^6. Despite the difference in Reynolds number, agreement between the data sets is generally very good, although those of Torres and Mueller [5] and Shields and Mohseni [9] tend to overshoot the rest of the data sets at high angles of attack. The contribution of the potential lift to the total lift increases significantly compared to AR = 0.5. Larson's prediction shows good agreement with experiment when all three lift components are included. Purvis' predictions, as seen for AR = 0.5, show best accord with experiment when only the potential and side edge vortex lift constituents are used.

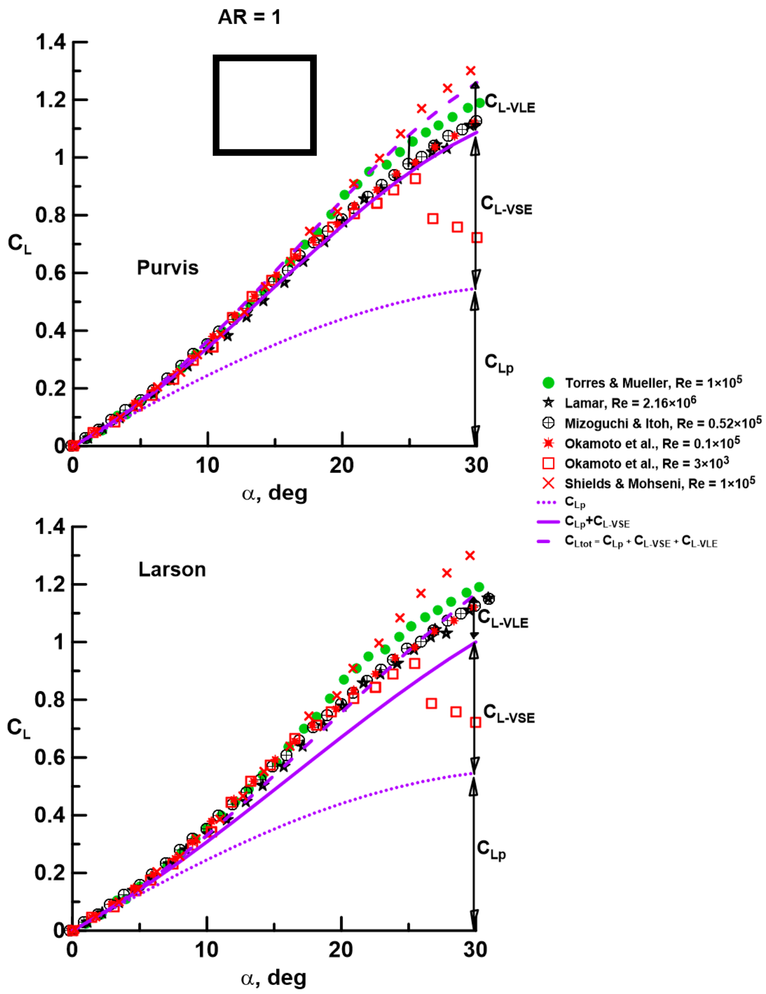

Figure 3. Lift coefficient correlation of methods of Purvis and Larson with experimental data for an AR = 1 rectangular flat plate wing. Okamoto et al. data from Ref. [2].

Increasing plate aspect ratio to 1.5, see Figure 4, shows a lift curve that is fairly linear. Considering the C_L decomposition, the majority of lift produced by the wing is associated with attached flow potential lift. The contribution of the side edge vortex lift is notably reduced compared to AR = 0.5. The Larson/Lamar prediction shows agreement with experiment when all three lift constituents are included, while, as seen for AR = 0.5 and 1, Purvis' estimates are closest to experiment when only the potential and side edge vortex lift are accounted for.

Aspect ratio = 3 plates show a lift curve that is essentially linear (see Figure 5). Any contribution of the side edge or leading edge vortex lift is small, leaving an essentially linear lift curve slope. The inclusion of leading edge vortex lift in Larson's estimates causes a moderate overprediction of lift, while Purvis' estimates are consistently best with the inclusion of only the potential and side edge vortex lift contribution.

The overarching result from Figures 2–5 is that Purvis' method is consistent and shows close accord with experiment when only the potential and side edge vortex lift is considered. The approach of Larson/Lamar requires the inclusion of the leading edge vortex lift in some cases and its omission in others for best agreement with experimental data. Considering that the actual physical realization of the leading edge vortex lift under steady state conditions is unlikely, the approach of Purvis appears to be that which is most consistent and physically justifiable in terms of the modeling of thin flat plate rectangular airfoils.

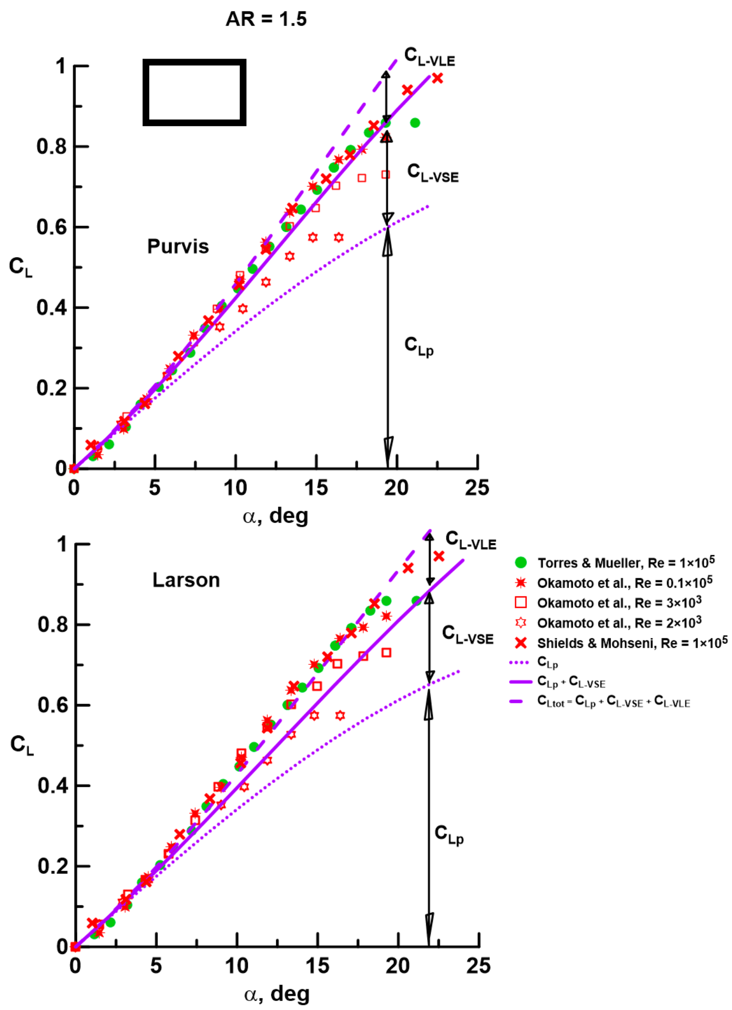

Figure 4. Lift coefficient correlation of methods of Purvis and Larson with experimental data for an AR = 1.5 rectangular flat plate wing. Okamoto et al. data from Ref. [2].

Torres and Mueller [5] extracted the location of the center of pressure of some of their test cases to show the location of the resultant force associated with the potential flow and vortex lift constituents. Figure 6 shows data from Ref. [5] in addition to those calculated using Lamar's data [11] for an AR = 1 rectangular wing. The center of pressure was calculated as the moment reference ($\frac{1}{4}$ chord) less the ratio of C_m to C_L (i.e., $=\frac{1}{4} - C_m/C_L$) or C_m to $C_{L\text{-VSE}}$. For analysis, the potential flow lift was assumed to act at the quarter chord. The estimated location of the center of pressure for all (i.e., the result $X_{C_{L\text{-TOT}}}/c$) lift components is seen to be in reasonable agreement with Lamar's and Torres and Mueller's data. As long as the non-linear lift component is negligible (i.e., low α), the center of pressure is noted to be close to the quarter chord. As shown in Figure 3, non-linearity of the lift curve becomes pronounced for $\alpha > 10$ degrees, coincident with the aft shift of the center of pressure in Figure 6. The calculation of the point of action of the side edge vortex lift ($X_{C_{L\text{-VSE}}}/c$) indicates that it progressively moves aft with an increasing angle of attack—a consequence of the increasing size, strength, and upper surface footprint of the side edge vortices. The strength of these vortices increases streamwise as more vorticity moves into the structure. Increasing the angle of attack would strengthen the side edge vortices as the differential loading between the windward and leeward wing surfaces intensifies.

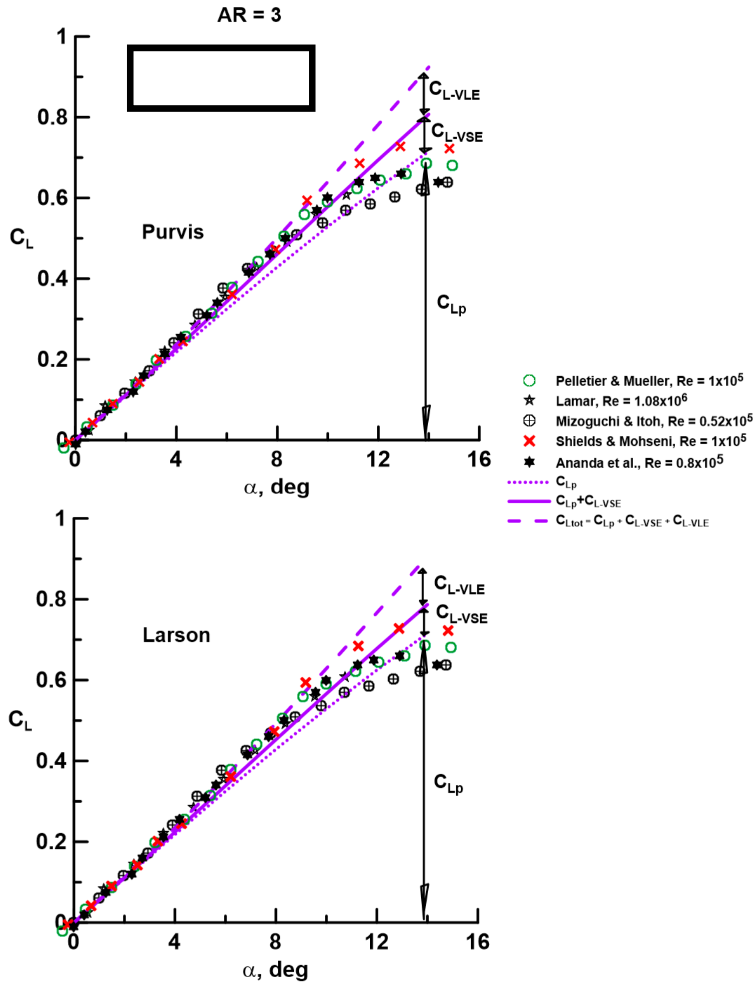

Figure 5. Lift coefficient correlation of methods of Purvis and Larson with experimental data for an AR = 3 rectangular flat plate wing (Ananda et al. data from Ref. [25]).

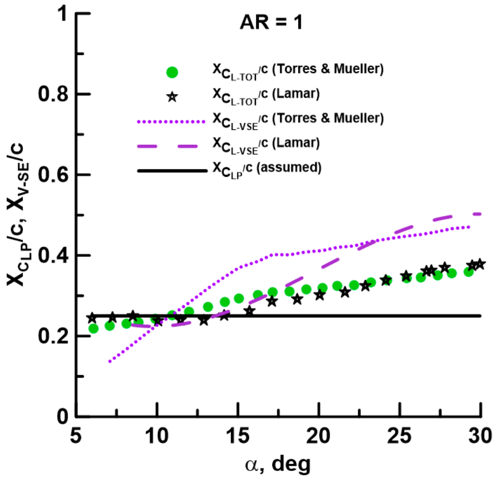

Figure 6. Estimated location of the center of pressure of the attached flow potential lift and side edge vortex lift components, AR = 1.

4. Conclusions

Experimental data for low aspect ratio rectangular flat plate wings are examined in terms of the lift constituents developed by the wings. As such, two methods of analysis are employed, both based on the leading edge suction analogy. The first method is closely allied with Polhamus' formulation, as extended by Lamar, while the second formulation is that of Purvis. The largest discrepancy between the two approaches is in the estimation of the side edge vortex lift: Purvis' estimates are significantly higher than those of Lamar. In terms of experimental data comparison, Purvis' method is the most consistent in terms of agreement with experiment when only the attached flow potential and side edge vortex lift is included. Lamar's approach requires the inclusion of the leading edge vortex lift in some cases and exclusion in others for the best agreement with experiment. As the realization of the leading edge vortex lift under steady state conditions for rectangular wings is physically unlikely, the approach of Purvis may be considered as representative in terms of flow physics and accuracy.

Funding: This research received no external funding.

Institutional Review Board Statement: Not applicable.

Informed Consent Statement: Not applicable.

Data Availability Statement: No new data were created for this publication.

Conflicts of Interest: The author declares no conflict of interest.

Abbreviations

The following abbreviations are used in this manuscript.

AR	aspect ratio
C_D	drag coefficient
C_{Do}	zero lift drag coefficient
C_L	lift coefficient
C_{LP}	potential lift coefficient
$C_{L\text{-}LE}$	leading edge vortex lift coefficient
$C_{L\text{-}SE}$	side edge vortex lift coefficient
$C_{L\text{-}tot}$	total lift coefficient
C_m	pitching moment coefficient
c	chord
K_P	potential constant
$K_{V\text{-}LE}$	leading edge vortex lift constant/coefficient
$K_{V\text{-}SE}$	side edge vortex lift constant/coefficient
X	chordwise location of center of pressure
Λ	leading edge sweep angle

References

1. Mizoguchi, M.; Kajikawa, Y.; Itoh, H. Aerodynamic Characteristics of Low-Aspect-Ratio Wings with Various Aspect Ratios in Low Reynolds Number Flows. *Trans. Jpn. Soc. Aero. Space Sci.* **2016**, *59*, 56–63. [CrossRef]
2. Okamoto, M.; Sasaki, D.; Kamikubo, M.; Fujii, R. Disappearance of Vortex Lift in Low Aspect Ratio Wings at Very Low Reynolds Number. *Trans. Jpn. Soc. Aero. Space Sci.* **2019**, *62*, 310–317. [CrossRef]
3. Lamar, J.E.; Gloss, B.B. Subsonic Aerodynamic Characteristics of Interacting Lifting Surfaces with Separated Flow Around Sharp Edges Predicted by a Vortex-Lattice Method. NASA TN D-7921. 1975. Available online: https://ntrs.nasa.gov/citations/19750023950 (accessed on 8 May 2023).
4. Pelletier, A.; Mueller, T.J. Low Reynolds Number Aerodynamics of Low Aspect Ratio Thin/Flat/Cambered Plate Wings. *J. Aircr.* **2000**, *37*, 825–832. [CrossRef]
5. Torres, G.; Mueller, T.J. Low Aspect Ratio Wing Aerodynamics at Low Reynolds Numbers. *AIAA J.* **2004**, *42*, 865–873. [CrossRef]
6. Okamoto, M.; Yasuda, K.; Azuma, A. Aerodynamic Characteristics of the Wings and Body of a Dragonfly. *J. Expt. Biol.* **1996**, *199*, 281–294. [CrossRef]
7. Larson, E.S. Sharp Edged Rectangular Wing Characteristics. *J. Aircr.* **1981**, *18*, 895–896. [CrossRef]
8. Mizoguchi, M.; Itoh, H. Effect of Aspect Ratio on Aerodynamic Characteristics at Low Reynolds Numbers. *AIAA J.* **2013**, *51*, 1631–1639. [CrossRef]
9. Shields, M.; Mohseni, K. Effects of Sideslip on the Aerodynamics of Low-Aspect-Ratio Low-Reynolds-Number Wings. *AIAA J.* **2012**, *50*, 85–99. [CrossRef]
10. Polhamus, E.C. A Concept of the Vortex Lift of Sharp-Edge Delta Wings Based on a Leading-Edge-Suction Analogy. NASA TN D-3767. 1966. Available online: https://ntrs.nasa.gov/citations/19670003842 (accessed on 8 May 2023).

11. Lamar, J.E. Extension of the Leading-Edge Suction Analogy to Wings with Separated Flow Around the Side Edges at Subsonic Speeds. NASA TR R-428. 1974. Available online: https://ntrs.nasa.gov/citations/19740026346 (accessed on 8 May 2023).
12. Traub, L.W. Extending the Leading Edge Suction Analogy to Non-Slender Delta Wings. *J. Aircr.* **2018**, *55*, 2174–2177. [CrossRef]
13. Er-El, J.; Yitzhak, Z. Experimental Examination of the Leading-Edge Suction Analogy. *J. Aircr.* **1988**, *25*, 195–199. [CrossRef]
14. Traub, L.W. Effects of Anhedral and Dihedral on a 75-deg Sweep Delta Wing. *J. Aircr.* **2000**, *37*, 302–312. [CrossRef]
15. Luckring, J.M. The Discovery and Prediction of Vortex Flow Aerodynamics. *Aero. J.* **2019**, *123*, 729–803. [CrossRef]
16. Sathaye, S.S. Lift Distributions on Low Aspect Ratio Wings at Low Reynolds Numbers. Master's Thesis, Worcester Polytechnic Institute, Worcester, MA, USA, 2004.
17. Eldredge, J.D.; Jones, A. Leading-Edge Vortices: Mechanics and Modeling. *Annu. Rev. Fluid Mech.* **2019**, *51*, 75–104. [CrossRef]
18. Jardin, T.; Choi, J.; Colonius, T. An empirical correlation between lift and the properties of leading-edge vortices. *Theor. Comput. Fluid Dyn.* **2021**, *35*, 437–448. [CrossRef]
19. Hoerner, S.F.; Borst, H.V. Fluid-Dynamic Lift. In *Hoerner Fluid Dynamics*; Mrs. Liselotte A. Hoerner: Brick Town, NJ, USA, 1975.
20. Traub, L.W.; Coffman, C. Efficient Low Reynolds Number Airfoils. *J. Aircr.* **2019**, *56*, 1987–2003. [CrossRef]
21. McCullough, G.B.; Gault, D.E. Examples of Three Representative Types of Airfoil Section Stall at Low Speed. NACA TN 2502. 1951. Available online: https://ntrs.nasa.gov/citations/19930083422 (accessed on 8 May 2023).
22. Helmbold, H.B. *Der Unverwundene Ellipsenflugel als Tragende Flache*; der Deutschen Luftfahrtforschung. R. Oldenbourg: Munich, Germany, 1942.
23. Purvis, J.W. Analytical Prediction of Vortex Lift. *J. Aircr.* **1981**, *18*, 225–230. [CrossRef]
24. Jones, R.T. Correction of the Lifting-Line Theory for the Effect of the Chord. NACA TN 817. 1941. Available online: https://ntrs.nasa.gov/citations/19930085047 (accessed on 8 May 2023).
25. Ananda, G.K.; Sukumar, P.P.; Selig, M.S. Measured Aerodynamic Characteristics Of Wings at Low Reynolds Numbers. *Aerosp. Sci. Technol.* **2015**, *42*, 392–406.